

Drying Simulated Advanced Gas Reactor Fuel: Proving the Concept – 17637

James Goode *, David Harbottle *, Bruce Hanson *

* School of Chemical and Process Engineering, University of Leeds, Woodhouse Lane, Leeds, LS2 9JT

ABSTRACT

Spent Nuclear Fuel (SNF) reprocessing is due to cease in the UK in 2018 and a new interim storage method may be required if it is found that pond storage is not viable beyond the 25 year period which is currently understood to be safe. Dry storage has been used elsewhere in the world for zircaloy and aluminium clad fuel and has been proposed for use in the UK, however since the UK's fuel is predominantly stainless steel (SS) clad, testing will need to be carried out to ensure that drying methods are suitable. This will require representative samples for macro scale drying tests. To date, little long term stored fuel has been examined. As a result, work has been carried out to try and ascertain whether the corrosion associated with long term storage leads to significant bound water and whether through wall cracks can be formed in intact lengths of SS tube.

It was found that unlike an aluminium simulant, corroded SS showed no sign of water loss as a result of oxide dehydration during controlled drying by thermogravimetric analysis, and consequently bound water could be disregarded. It was also found that through wall cracks could be produced in an intact length of SS tube which would be suitable for macro scale drying tests.

Some initial macro scale drying tests have been carried out using an alternative test piece with preformed cracks, and three distinct drying regimes to complete dryness have been detected.

INTRODUCTION

SNF from the UK's Advanced Gas Reactors (AGR) has traditionally been reprocessed. However, reprocessing is due to cease in 2018[1] with direct disposal to a Geological Disposal Facility (GDF). This is not envisaged being available until 2075 hence an interim storage method is required. The current NDA plan is to continue pond storage of AGR fuel until at least 2038, since experience has shown that AGR fuel can be safely stored in a caustic dosed pond for up to 25 years[2]. However, there is not yet any definitive plan for storage of fuel for the remaining 35 years. If it is found that prolonged pond storage is not viable one option that is being considered is dry storage[3].

Dry storage has been used successfully for Zircaloy clad LWR and aluminium clad research reactor fuel however AGR fuel is stainless steel clad hence further work is required to confirm the suitability of dry storage[4].

A key part of dry storage of spent fuel is the ability to adequately dry the fuel. Both vacuum drying and forced gas drying have been used commercially to dry LWR SNF[5], and a drying rig (see Figure 2) has been constructed to allow the two methods to be compared and their suitability for drying AGR fuel ascertained. Before this can commence there is a need to produce samples that are representative of fuel following long term pond storage. Only a limited amount of post storage examination (PSE) of spent AGR fuel has taken place so little is known of the condition of fuel following long term caustic pond storage.

Two forms of water were identified as being of possible concern when drying fuel[5]; bound and trapped water. Water may be present as adsorbed or chemically bound water on the surface oxide and the authors felt it was necessary to confirm the significance of such water. The small amount of PSE that has been undertaken has primarily taken place on failed fuel. This has shown that failures have been a result of combined intergranular corrosion (IGC) and stress corrosion cracking (SCC) and that such cracks may pass through the cladding wall[6]. The worst case scenario is a pin which has become flooded through such a crack after decades of pond storage trapping water inside since this would provide the greatest drying challenge. Consequently it is necessary to be able to produce cracks of similar morphology in an intact length of tube so that macro drying tests are able to assess the ease with which water can be removed through such cracks. The work described below establishes the significance of bound water, shows how a cracked length of SS tubing may be produced and shows the results of some initial macro scale drying tests.

EXPERIMENTAL METHODS

Assessment of Bound Water

Preliminary work was completed with a small number of aluminium samples to represent aluminium clad fuel. It is known that aluminium has a water containing oxide layer which can be dehydrated upon heating[7]. Since aluminium clad fuel has been successfully dry stored it was felt that aluminium would be a suitable material to use to ascertain whether TGA was suitable for measuring the loss of bound water from SNF. These samples were ~3 mm square and were cut from a sheet of 1 mm 1050 aluminium sheet. These samples were washed in acetone in an ultrasonic bath and rinsed with demineralized water to remove any surface contamination before being submerged in demineralized water for a period of 6 weeks leading to visible surface oxidation. These samples were then exposed to a

controlled drying process by thermogravimetric analysis (TGA). The drying profile consisted of heating from 40°C to 400°C at a rate of 10°C min⁻¹ under a flow of nitrogen at 50 mL min⁻¹. The samples were loaded wet into the TGA.

Further tests were carried out using sections of a similar size cut from an unirradiated fuel pin obtained from NNL (AGR fuel cladding). AGR cladding is made of a specialist grade of SS containing 20 wt% Cr, 25 wt% Ni with the addition of 1 wt% Nb[8] to prevent thermal sensitisation. A fuel pin has an outside diameter of 14.5 mm and a wall thickness of ~400 µm. All samples were washed in acetone before use.

The samples were treated in two ways. A set of three samples were held in a boiling solution of 65% nitric acid and 1% potassium dichromate for 1 hr (referred to as HNO₃). This treatment was intended to induce IGC in the samples[9]. Samples were placed into demineralized water between treatment and drying to prevent natural drying in. A second set of three samples were placed in an autoclave containing demineralized water dosed to pH 11.4 at room temperature. The autoclave was then heated to 200°C and 15 BarG and the samples were held for 4 weeks (referred to as NaOH). This was carried out to approximate samples which had spent many years in a caustic dosed pond by increasing the reaction kinetics. Following the treatment the samples were placed in demineralized water until testing was carried out. A third set of samples in the as received (AR) state were also held in demineralized water for two weeks as a control.

The three samples of SS cladding were then dried by TGA using a heating profile of 50–500°C at a rate of 10°C min⁻¹ under a flow of nitrogen at 50 mL min⁻¹. The samples were loaded into the TGA instrument wet to prevent atmospheric drying due to evaporation before the controlled drying process.

Cracked Sample Production

SCC occurs as a result of a combination of tensile stress (σ) and a corrosive media[10]. Numerous studies have induced SCC in austenitic SS with the use of boiling magnesium chloride solutions[11]. An initial SCC sample was produced by cutting a ring from a length of 304 SS tube with 15 mm outside diameter and 1.5 mm wall thickness. This small ring was around 10 mm in length. The ring was annealed in argon at 1100°C for 60 min before quenching and was then sensitised at 650°C for 24 hr. Following this the ring was bolted between two plates to create a compression ring as seen in **Error! Reference source not found.** The compression ring was boiled in 42 wt% MgCl₂ for 4 weeks. The metal was insulated from the compression plates with PTFE to prevent any galvanic effects. Following this a 60 mm length of the same tube was treated in the same manner. Traditionally σ is induced by compressing an incomplete C-ring which induces σ throughout the outer wall of the sample encouraging SCC in this area[12].

The use of a complete ring in a compression test leads to σ on the outer surface of the ring at position B and D and on the inner surface at A and C and it is at these positions that stress corrosion cracks are expected to be formed.

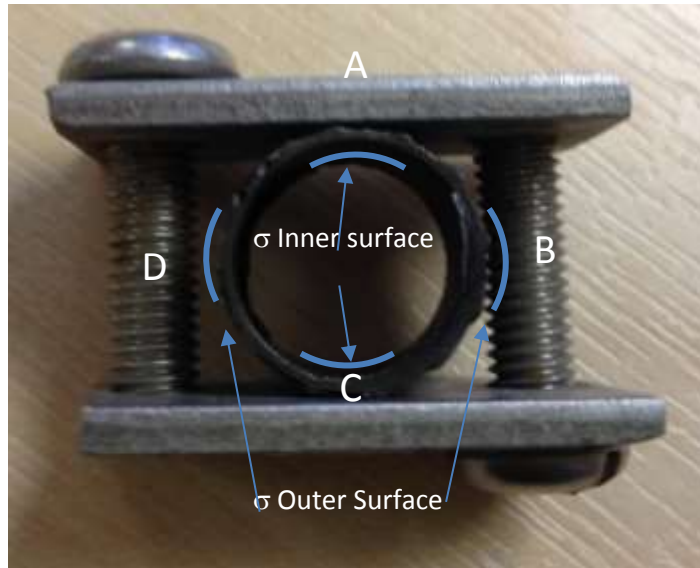


Figure 1. Compression ring apparatus used to produce SCC.

Macro Scale Drying Tests

A pilot-scale drying rig was constructed to carry out macro scale drying tests. This is shown in Figure 2 along with the drying rig P&ID in Figure 3. The drying rig is designed to allow both vacuum and flowed gas drying so that the two drying methods can be compared under controlled environments. K-type Thermocouples (TC) were placed at numerous positions around the rig and temperature measurements were continuously logged. Two thermocouples were inside the vessel one to record the vessel gas temperature and a second flexible thermocouple which may be attached to a sample, to monitor surface temperature. A further TC was placed on the vessel base. The vessel pressure was continuously logged with an Omega Engineering PX309 pressure transducer (0 - 2 BarA range). Finally, a Bronkhorst EI-flow mass flow meter was fitted in-line to the vacuum source. Vacuum was supplied with an Edwards E2M2 pump. Gas is can also be pumped around the system with a TCS D10K micro-pump and through a Watlow Cast-X 1000 circulation heater to provide warm gas to the vessel.

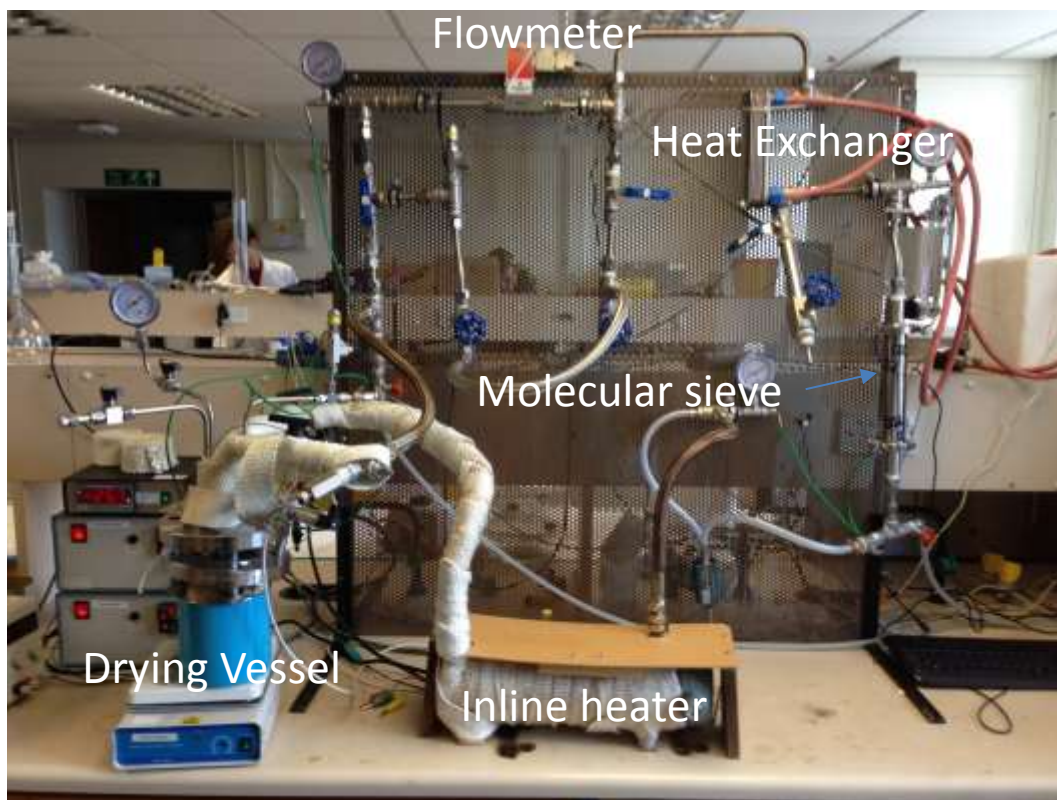


Figure 2. The pilot-scale drying rig.

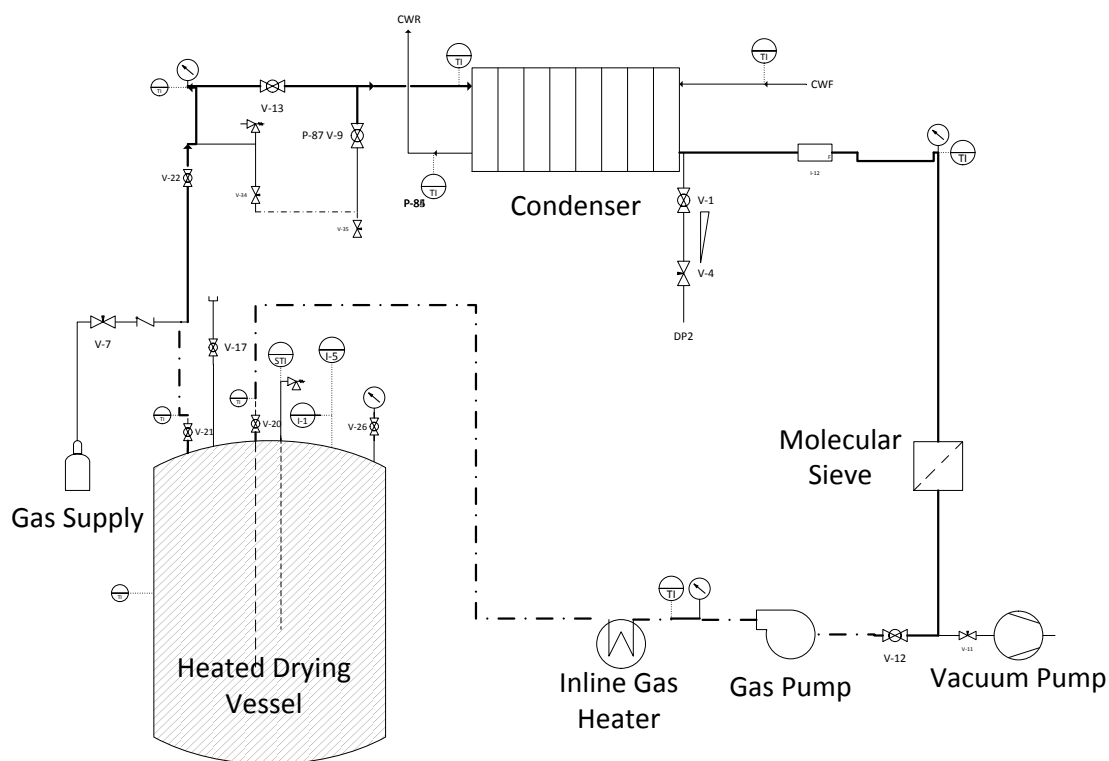


Figure 3. P&ID of drying rig.

RESULTS AND DISCUSSION

Assessment of Bound Water

The TGA results for the aluminium samples are shown in Figure 4. There is a large initial mass drop as the temperature increases to around 100°C as the free water is removed from the sample. A further much smaller reduction in mass is evident at ~250°C. The second mass change is due to the dehydration of the bayerite ($\text{Al}_2\text{O}_3 \cdot 3\text{H}_2\text{O}$) oxide layer formed on aluminium when held in water to form boehmite ($\text{Al}_2\text{O}_3 \cdot \text{H}_2\text{O}$) [7].

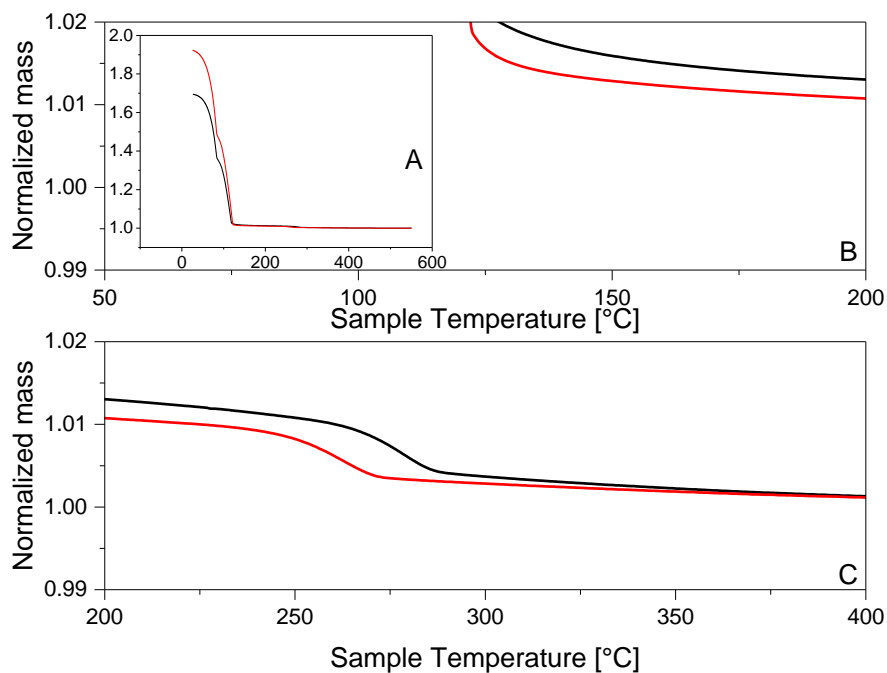


Figure 4. TGA curves for two aluminium samples. The inset (A) shows the full drying curve with high initial mass loss, and (B) and (C) show the sample drying on an enlarged scale to clearly identify sample dehydration.

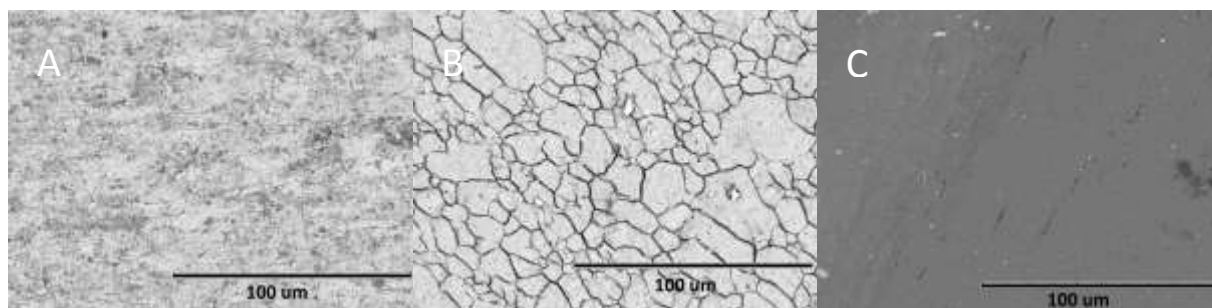


Figure 5. Cladding in the as received state (A), after undergoing IGC in nitric acid solution (B), and after being held in caustic dosed water (C).

Figure 5 shows SEM images of the fuel cladding samples which were dried by TGA. It can be seen that the sample which had been immersed in the boiling nitric acid solution (B) shows evidence of IGC unlike the AR sample (A) or sample immersed in caustic dosed water (C), although the caustic dosed water sample did have a clear dark oxide layer on the surface which was visible with the naked eye and accounts for the darkness in the SEM image.

Figure 6 shows the TGA curves for the samples of SS fuel cladding. Only two of the three samples in each set are shown in the interests of clarity however the behaviour of the third sample was similar. Once again there is a large initial mass drop as the free water in the crucible is removed, however there is no mass change at higher temperatures (unlike the aluminium sample), confirming that surface bound water is either negligible (below the detection limit of the measurement technique) or not present. There is no difference in behaviour as a result of the different material treatment methods.

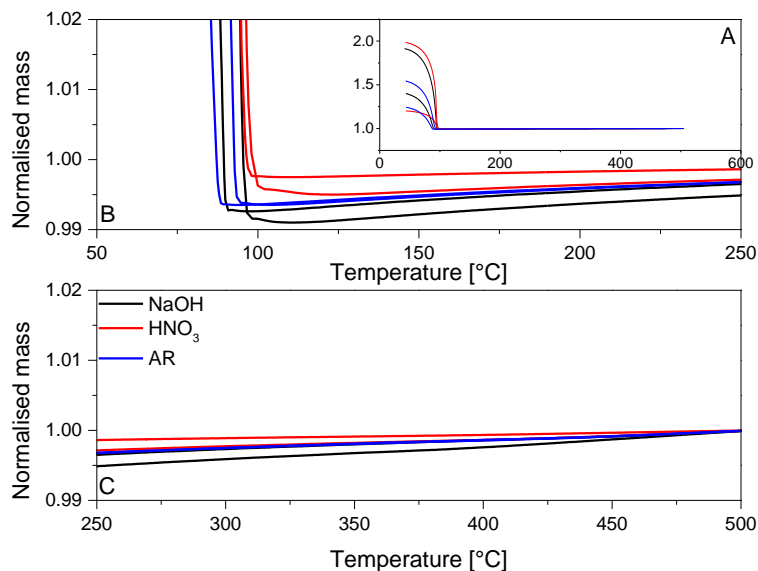


Figure 6. TGA for the drying of SS samples. The inset (A) shows the full drying curve with high initial mass loss, and (B) and (C) show the sample drying on an enlarged scale, with no observable sample dehydration at higher temperatures.

Cracked Sample Production

Having confirmed that bound water on a SS sample is negligible it was necessary to produce a tube that contained through wall cracks. Figure 7 shows the small 304 SS ring after SCC (the image has been rotated by 90° relative to **Error! Reference source not found.**). The ring was cut in half to increase the visible surface area. A relatively large crack is visible at position A on the sample shown on the right. This can be seen to be developing from the inside which was under tensile stress. A further smaller crack was also found at D on the sample shown on the left. Again this crack develops from the surface under tensile stress, in this case the outside. These results show that it is possible to develop SCC cracks with this method although it is not confirmed that such cracks will pass through the tube wall.

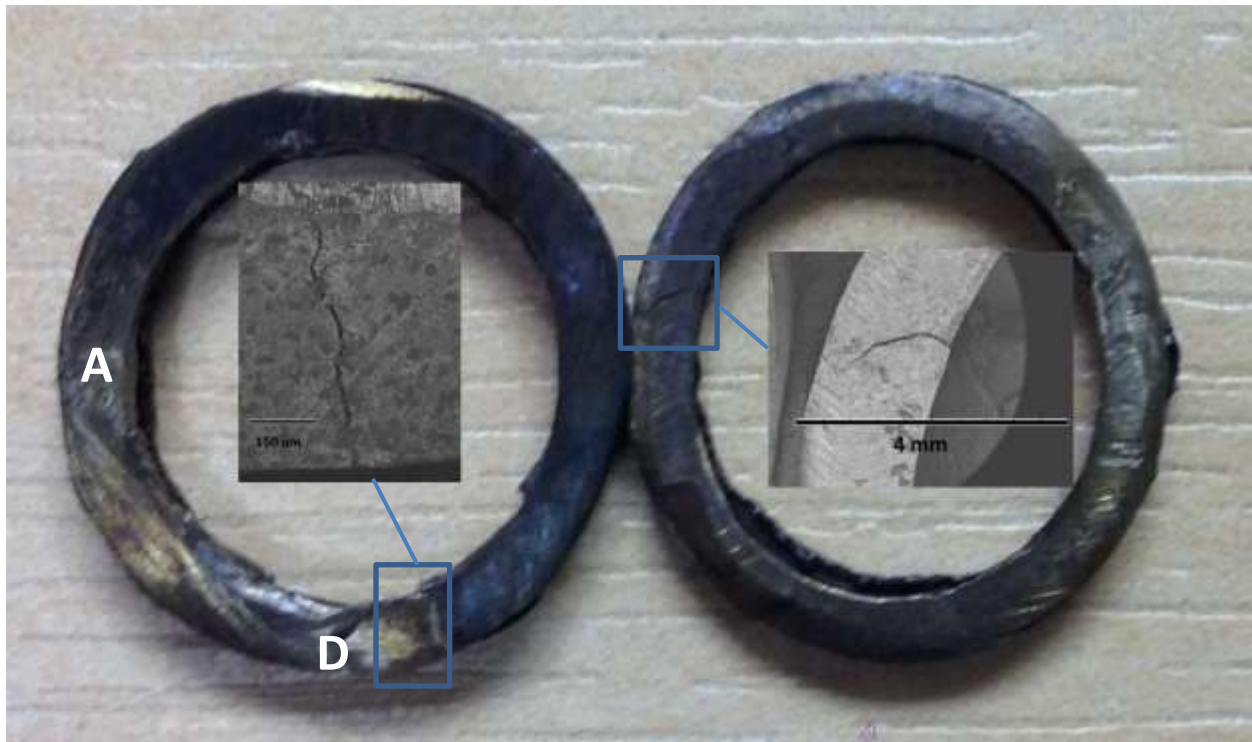


Figure 7. Small 10 mm ring of 304 SS following compression and SCC (image rotated by 90° relative to Figure 1).

Figure 8A and B shows cracks that formed along the length of the 60 mm 304 SS tubing following sensitization and boiling in $MgCl_2$. In this sample cracks that ran the length of the tube were visible at both the B and D positions externally (refer to Figure 1 for locations). Internally it was possible to see cracks at both the A and C positions. While it could not be confirmed that the cracks passed fully through the cladding, it was felt that due to the length of the cracks it was likely that at some point a through wall crack would exist which was not visible to the naked eye and that the tube should be used in some initial macro drying tests. This required fitting a twin ferrule compression fitting to the tube. This was complicated due to the deformation caused by the compression ring however while the compression fitting was added to the test sample cracks opened up in several places to produce through cladding cracks, as can be seen in Figure 8D.

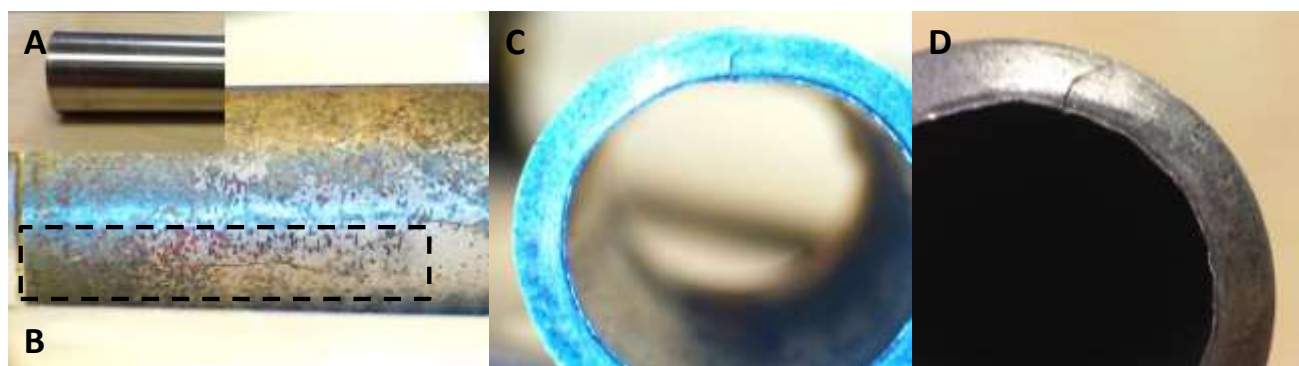


Figure 8. Pre- (A) and post-treatment (B, C) images of the 60 mm 304 SS tube showing initial cracks formed along the length of the sample. D shows an extended crack following manipulation to fit cap.

Macro Scale Drying Rig

The initial drying tests which are shown in Figure 10 used the test piece (TP) shown in Figure 9 since the cracked SS was still in production. This TP consists of a length of 15 mm outside diameter acrylic tube with 1 mm walls. The tube was carefully compressed to produce a crack running the length of the TP. The heater on the vessel walls was set to 30°C and the vacuum pump was run at full power for the duration of the test. Each test lasted around 1 hr at the end of which the TP was removed, weighed and replaced for another test. The rate at which water was lost from the test piece was calculated from the mass change to give a pseudo drying rate. A total of 8 tests were required to remove all of the water and four distinct behaviours were observed in three different drying regimes. Only a selection of the eight tests are shown to prevent repetition.



Figure 9. Test piece (TP) used for pilot-scale drying tests. The crack is visible as a white line towards the bottom of the sample.

The key data output is in the form of data plots showing how the various logged parameters change with time. The drying data is shown in Figure 10.

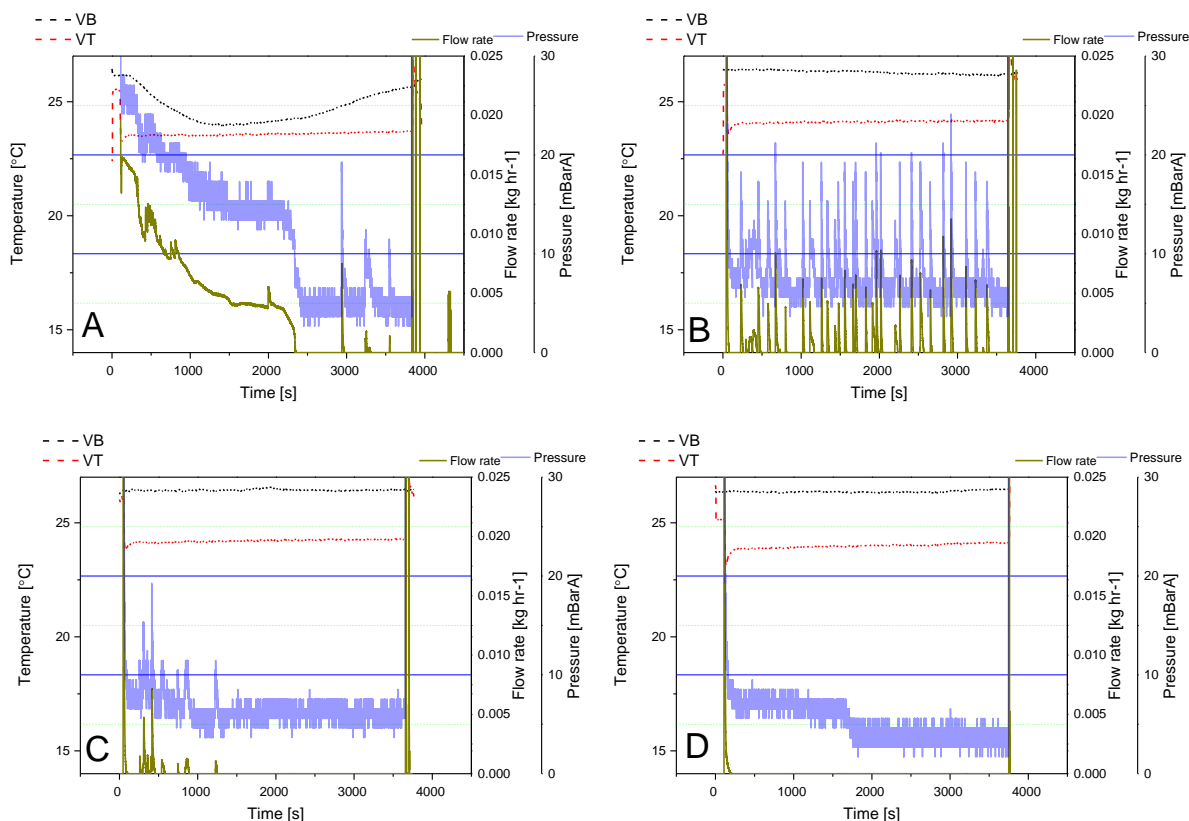


Figure 10. Data output from pilot-scale drying tests. Test 1 (A), Test 3 (B), Test 4 (C) and Test 8 (D).

For Test 1 the gas temperature (VT) remains constant throughout the test. The temperature of the vessel base (VB) is slightly below that of the heated walls. The pressure and flow rate drop rapidly as the vessel is initially evacuated. Pressure and flow begin to plateau around $t = 100$ s ($P = 28$ mBarA). VB drops as energy is used to boil the water. It can be seen that the pressure and flow rate follow each other closely. After around 2500 s there is another significant drop in pressure (from 15 mBarA) and flow rate with the flow rate now approximately zero and the pressure averaging around 7 mBarA (but with several significant spikes), and VB begins to return to the starting temperature. The overall drying rate for Test 1 was 0.91 mg s^{-1} .

The initial high flow rate is believed to be due to the ejection of water from the TP at the beginning of the test. When the test begins the unavoidable air space left in the TP expands as the vessel is evacuated forcing water out through the crack. This water then boils away from in the vessel base to give a high flow rate and pressure. The first change in drying regime occurs when this water is boiled off entirely leading to a drop in flow rate and pressure.

During this period the boiling of water in the TP leads to a slow increase in pressure inside the tube. This leads to occasional spikes in flow and pressure as slugs of water are pushed through the crack which flash to steam due to a pressure drop between inside the TP and the vessel itself.

The behaviour for Test 2 (not shown) was similar to that of Test 3 which can be seen in Figure 10B with the pressure averaging around 5 mBarA. There is no evident change in temperature in the remaining tests except for an initial sharp drop due to adiabatic cooling as the vacuum is applied. For both Tests 2 and 3 the drying rate was found to be 0.28 mg s^{-1} .

Test 4 (see Figure 10C) shows the transition to the final drying regime. This takes place as the level of water drops below the level of the cap. Once this happens it is no longer possible for slugs of water to be ejected. The spikes in pressure and flow rate are no longer observed but the pressure stays around 5 mBarA. The drying rate for Test 4 was lower again at 0.20 mg s^{-1} .

Tests 5, 6 and 7 (not shown) all behaved in the same manner as the second half of Test 4. The pressure remained constant at 5 mBarA and the flow rate appears to be zero as it is below the range of the flow meter. The drying rates for these tests had once again dropped to 0.14 , 0.13 and 0.14 mg s^{-1} , respectively.

The final behaviour is found in Test 8, as shown in Figure 10D. This is believed to occur as the final drops of water are removed at $\sim 1700 \text{ s}$, which is indicated by a drop in pressure to 3.5 mBarA. The drying rate for the entire test is now 0.09 mg s^{-1} .

CONCLUSION

TGA has been shown to detect mass loss from the dehydration of corroded aluminium as a simulant for aluminium clad fuel. Such fuels have been successfully dried and placed in dry storage.

Samples of SS AGR cladding have been treated to induce IGC which is known to be a failure mode and also in a manner which will broadly simulate long term storage in a caustic dosed pond.

These samples have then undergone TGA similar to the aluminium samples, as well as being compared with untreated cladding which has undergone the same controlled drying. None of these samples show any mass loss indicative of dehydration. While this does not prove that there is not a trace amount of bound water present, the data would suggest that the quantities of bound water held on the oxide layer of long term pond stored AGR fuel are low enough to be disregarded in terms of the macro scale drying tests planned, and for future dry storage of AGR SNF.

The use of C-rings and boiling magnesium chloride is known to induce SCC in sensitised stainless steels and is used in standard ASTM tests[12], [13]. The current research has shown that a modified method using intact tubes of SS and compression rings is also capable of producing cracks. This means that with the use of twin ferrule compression fittings it is possible to seal water inside a tube allowing drying tests to be carried out to ascertain the ease with which water can be removed through cracks under different drying conditions.

A pilot-scale drying rig has been developed, commissioned and tested. Early drying experiments have been carried out with a length of cracked acrylic tube, and the system data can be used to observe different drying regimes and the drying rates in the different drying regimes. Further tests will be carried out with lengths of cracked 304 SS tubing, and if possible cracked AGR cladding which is believed to be more representative of real long term stored AGR fuel.

REFERENCES

- [1] Nuclear Decommissioning Authority, "Oxide Fuels Preferred Options," Nuclear Decommissioning Authority, SMS/TS/C2-OF/001/Preferred Option, Jun. 2012.
- [2] J. Kyffin, "The technical case for interim Storage of AGR fuel and development of a programme of further work," presented at the Sustainable Nuclear Energy Conference, Manchester, 2014.
- [3] Independent NDA Research Board, "Review of NDA's Spent Fuels R&D Programme," NDARB016, Oct. 2014.
- [4] IAEA, "Survey of wet and dry spent fuel storage," IAEA, Vienna, IAEA-TECDOC-1100, Jul. 1999.
- [5] ASTM C-1553-Standard Guide for Drying Behaviour of SNF. .
- [6] J. Kyffin, "Technological Development to Support a Change in the United Kingdom's Strategy for Management of Spent AGR Oxide Fuel," in *Proceedings of the International Conference on Management of Spent Fuel from Nuclear Power Reactors*, Vienna, 2015.
- [7] J. W. Diggle and A. K. Vijn, "The Aluminium-Water System," in *Oxide and Oxide Films*, vol. 4, 4 vols., New York: Marcel Dekker Inc, 1976.

- [8] G. W. Horsley and J. A. Cairns, "The inhibition of carbon deposition on stainless steel by prior selective oxidation," *Appl. Surf. Sci.*, vol. 18, no. 3, pp. 273–286, 1984.
- [9] O. V. Kasparova, "The effect of boron and carbon on the structure and corrosion-electrochemical behavior of Kh20N20 austenitic stainless steel," *Prot. Met. Phys. Chem. Surf.*, vol. 49, no. 6, pp. 734–739, Nov. 2013.
- [10] NACE International, "Stress Corrosion Cracking (SCC)," *NACE International*. [Online]. Available: [https://www.nace.org/Corrosion-Central/Corrosion-101/Stress-Corrosion-Cracking-\(SCC\)/](https://www.nace.org/Corrosion-Central/Corrosion-101/Stress-Corrosion-Cracking-(SCC)/). [Accessed: 12-Jan-2017].
- [11] W. Wu, Y. Guo, H. Yu, Y. Jiang, and J. Li, "The Quantitative Effect of Mo and Cu on the Stress Corrosion Cracking and Pitting Corrosion Behavior of Ultra-Pure Ferritic Stainless Steels," *Int. J. Electrochem. Sci.*, vol. 10, no. 12, pp. 10689–10702, 2015.
- [12] ASTM International, "ASTM G38 - 01(2013) Standard Practice for Making and Using C-Ring Stress-Corrosion Test Specimens," 2007.
- [13] ASTM International, "ASTM G36 - 94(2013) Standard Practice for Evaluating Stress-Corrosion-Cracking Resistance of Metals and Alloys in a Boiling Magnesium Chloride Solution," 2007.